Electronic Supplementary Material (ESI) for Energy & Environmental Science.
This journal is © The Royal Society of Chemistry 2024

Supplementary information for

# Does trapped $O_2$ form in the bulk of $LiNiO_2$ during charging?

Mikkel Juelsholt[1]†, Jun Chen[1]†, Miguel A. Pérez-Osorio[1,2], Gregory J. Rees[1,2], Sofia De Sousa Coutinho[1,2], Helen E. Maynard-Casely[3], Jue Liu[4], Michelle Everett[4], Stefano Agrestini[5], Mirian Garcia-Fernandez[5], Ke-Jin Zhou[5], Robert A. House[1,2]*, Peter G. Bruce[1,2,6]*

1. Department of Materials, University of Oxford, Oxford, U.K.
2. Faraday Institution, Didcot, U.K.
3. Australian Nuclear Science and Technology Organisation, Kirrawee, New South Wales, Australia
4. Neutron Scattering Division, Oak Ridge National Laboratory, Oak Ridge, Tennessee, United States
5. Diamond Light Source, Harwell, U.K.
6. Department of Chemistry, University of Oxford, Oxford, U.K.

† These authors contributed equally

* Corresponding authors robert.house@materials.ox.ac.uk, peter.bruce@materials.ox.ac.uk

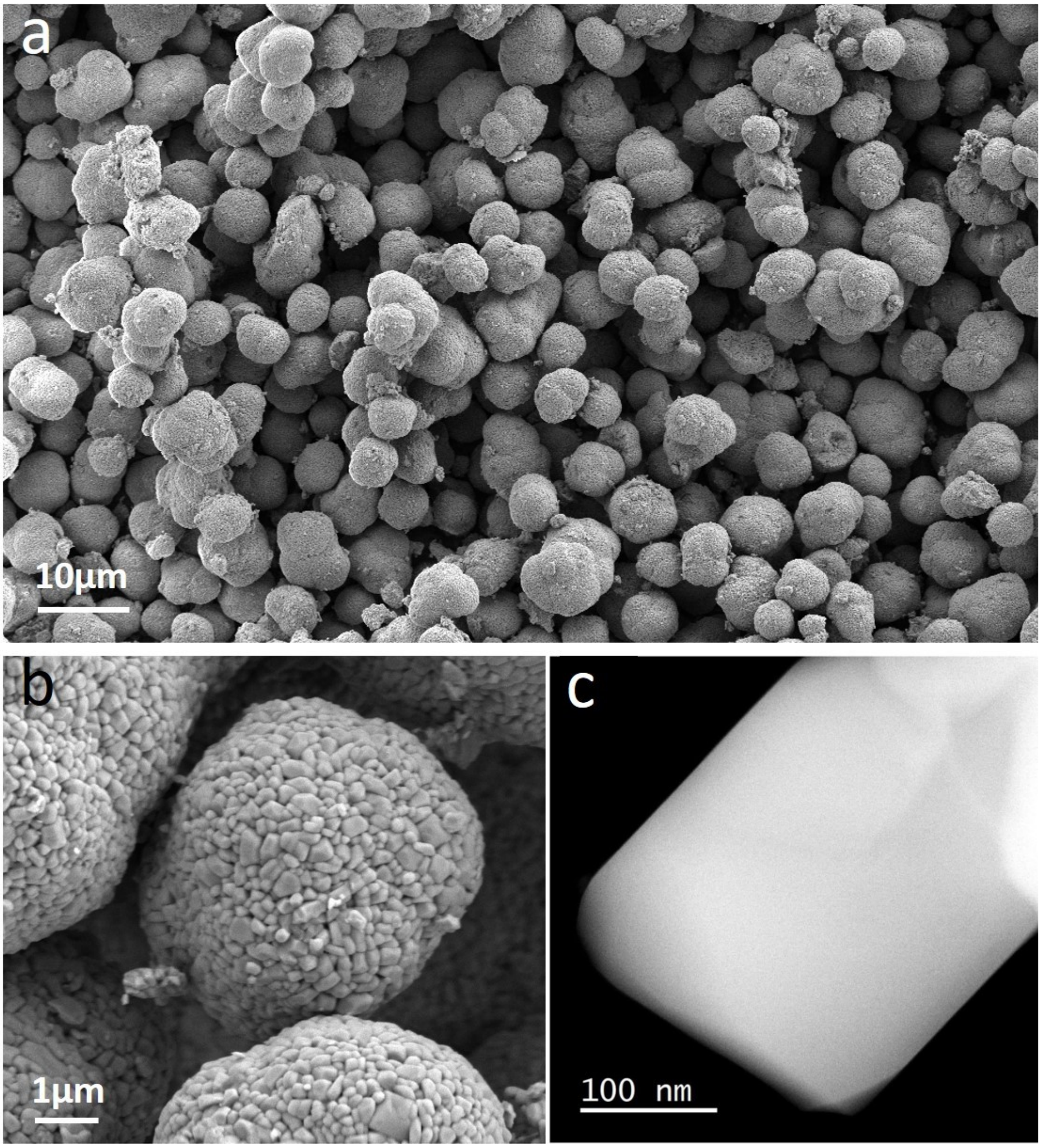


**Supplementary Figure 1.** (a,b) SEM images (c) HAADF-STEM images showing the particle morphologies and sizes.

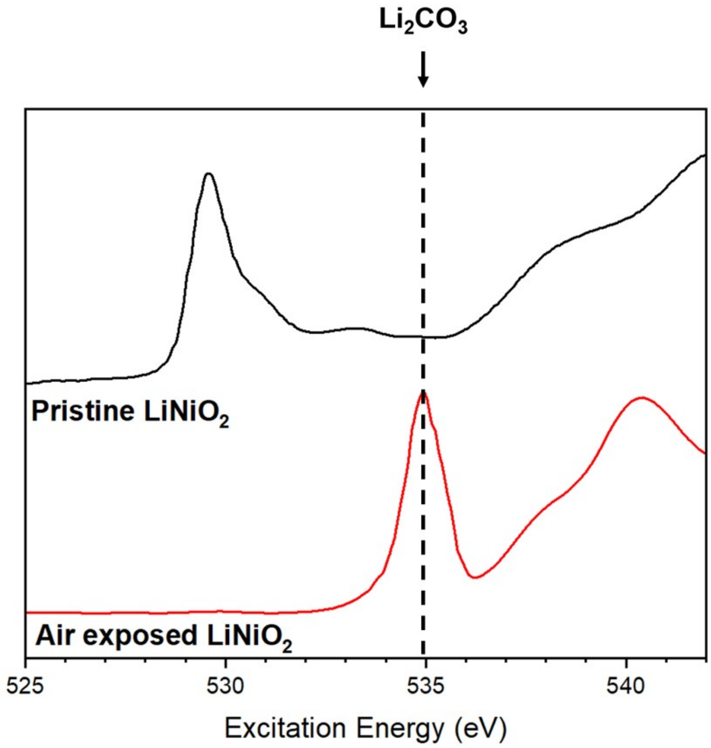


**Supplementary Figure 2. Comparison between** O K-edge XAS data of our sample in black and air-exposed $LiNiO_2$. The spectrums are adopted from [Green at al. '*Evidence for bond-disproportionation in $LiNiO_2$ from x-ray absorption spectroscopy'*, arxiv (2020)]. The peak at 535 eV arising from the presence of $Li_2CO_3$ is absent in our samples confirming clean surfaces and no air exposure.

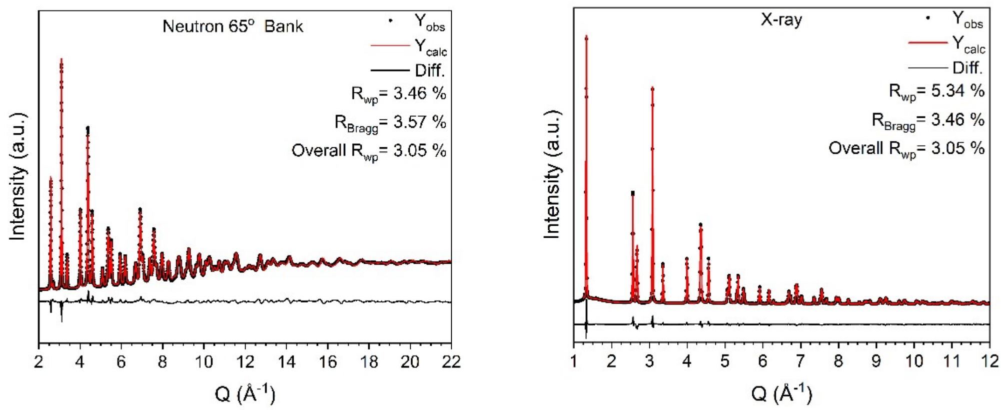


**Supplementary Figure 3:** Pristine $LiNiO_2$ Rietveld refinements of time-of-flight PND and PXRD.

**Supplementary Table 1:** Refined structural parameters for the pristine $LiNiO_2$.

| Space group | | | | | |
|---|---|---|---|---|---|
| R-3m | a | 2.87785(4) Å | c | 14.1998 (2) Å | |
| Atom | x | y | z | Occupancy | B |
| Li | 0 | 0 | 0 | 0.9559 (2) | 0.58 (2) Å$^2$ |
| Ni | 0 | 0 | 0 | 0.04424 (4) | 0.113 (1) Å$^2$ |
| Ni | 0 | 0 | 0.5 | 1 | 0.113 (1) Å$^2$ |
| O | 0 | 0 | 0.238 (4) | 1 | 0.488 (3) Å$^2$ |

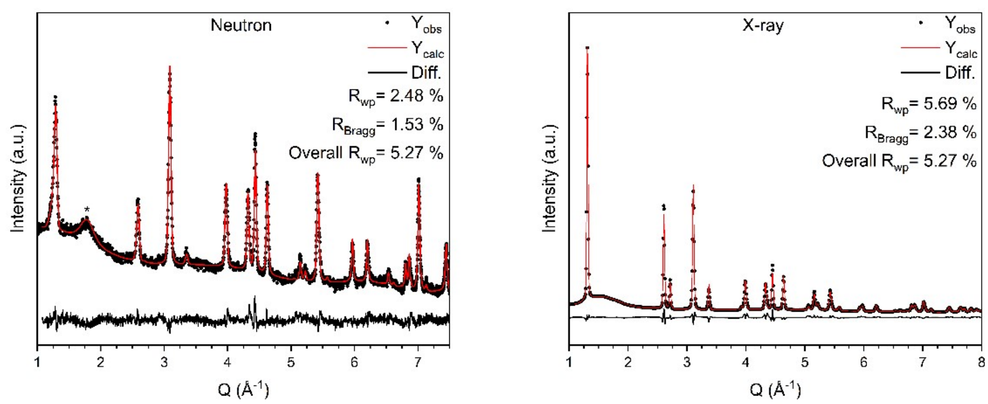


**Supplementary Figure 4:** $LiNiO_2$ charged to 4.1 V. Rietveld refinements of the neutron (left) and X-ray (right) diffraction data. The broad peak indicated with a star arises from the carbon in the electrode. The neutron diffraction data were measured with a constant wavelength of 1.622 Å.

**Supplementary Table 2:** Structural parameters for the combined refinement of $LiNiO_2$ charged to 4.1 V.

| Space group | | | | | |
|---|---|---|---|---|---|
| R-3m | a | 2.82653 (6) Å | c | 14.4179 (8) Å | |
| Atom | x | y | z | Occupancy | B |
| Li | 0 | 0 | 0 | 0.26 | 0.5 Å$^2$ |
| Ni | 0 | 0 | 0 | 0.029 (1) | 0.133 (3) Å$^2$ |
| Ni | 0 | 0 | 0.5 | 1 | 0.133 (3) Å$^2$ |
| O | 0 | 0 | 0.237 (3) | 1 | 0.575 (3) Å$^2$ |

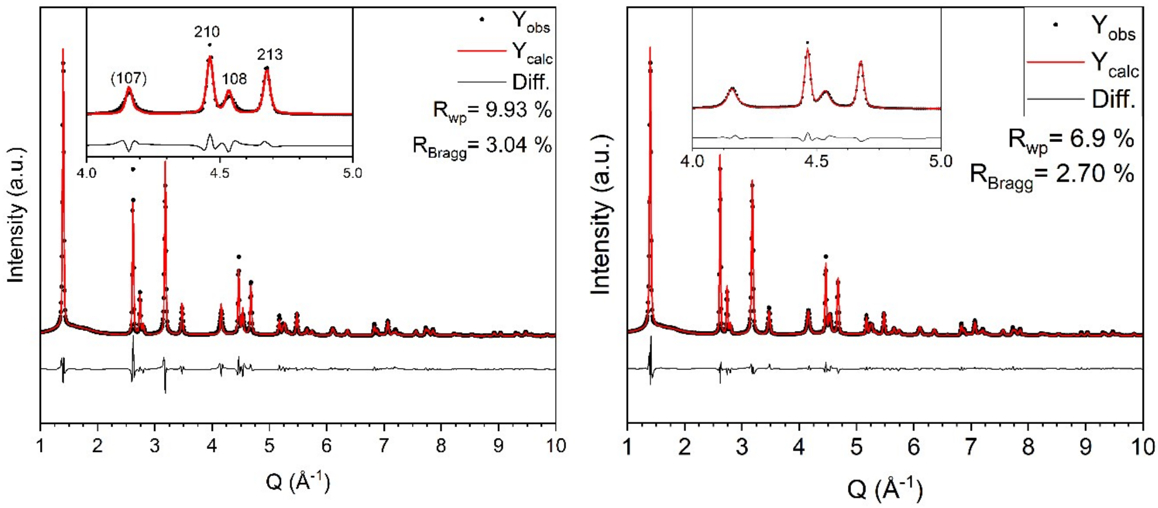


**Supplementary Figure 5**: (Left): X-ray Rietveld refinement with anisotropic atomic displacement parameters, but isotropic peak broadening for $LiNiO_2$ charged to 4.3 V. (Right)**:** X-ray Rietveld refinement with anisotropic atomic displacement parameters and anisotropic peak broadening for $LiNiO_2$ charged to 4.3 V. Same fit as shown in Figure 1c.*

**Supplementary Table 3:** Refined structural parameters for the $LiNiO_2$ charged to 4.3 V. Fit is shown in Figure 1c in the main text.

| Space group | | | | | |
|---|---|---|---|---|---|
| R-3m | a | 2.816 (1) Å | c | 13.474 (2) Å | |
| Atom | x | y | z | Occupancy | B |
| Li | 0 | 0 | 0 | 0.046 | 0.5 Å$^2$ |
| Ni | 0 | 0 | 0 | 0.024 (2) | See below |
| Ni | 0 | 0 | 0.5 | 0.921 (6) | See below |
| O | 0 | 0 | 0.237 | 1 | See below |
| Atom | $B_{11}$ | $B_{33}$ | $B_{12}$ | | |
| Ni | 0.034 (1) Å$^2$ | 4.02 (2) Å$^2$ | 0.017 (1) Å$^2$ | | |
| O | 1.49 (2) Å$^2$ | 3.55 (3) Å$^2$ | 0.74 (2) Å$^2$ | | |

We verified that the strongly anisotropic ADP in the refinement of the 4.3 V sample is a real structural effect by using total scattering with Pair Distribution Function (PDF) analysis. In the PDF, the occupancies and atomic positions are much less correlated with the ADPs, as shown in Supplementary Figure 12. The PDF confirms that the anisotropic ADPs are a real effect.

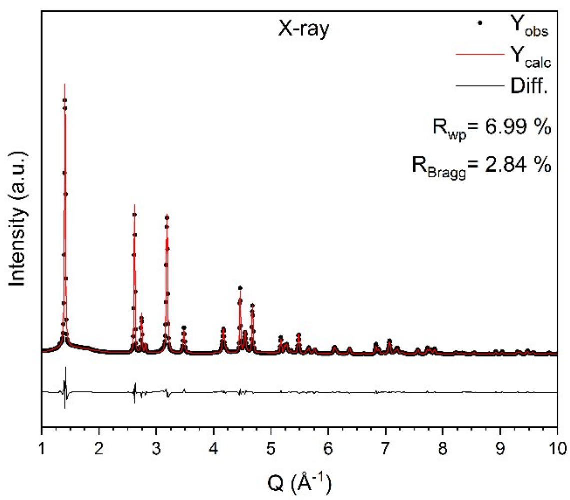


**Supplementary Figure 6:** Rietveld refinements of the X-ray diffraction obtained from $LiNiO_2$ charged to 5 V. Using the model also used in figure 1c in the main text.

**Supplementary Table 4**: Refined structural parameters for the $LiNiO_2$ charged to 5 V.

| Space group | | | | | |
|---|---|---|---|---|---|
| R-3m | a | 2.817 (1) Å | c | 13.417 (1) Å | |
| Atom | x | y | z | Occupancy | B |
| Li | 0 | 0 | 0 | 0.0 | 0.5 Å$^2$ |
| Ni | 0 | 0 | 0 | 0.026 (2) | See below |
| Ni | 0 | 0 | 0.5 | 0.926 (9) | See below |
| O | 0 | 0 | 0.238 | 1 | See below |
| Atom | $B_{11}$ | $B_{33}$ | $B_{12}$ | | |
| Ni | 0.034 (2) Å$^2$ | 3.55 (4) Å$^2$ | 0.017 (2) Å$^2$ | | |
| O | 0.71 (3) Å$^2$ | 3.43 Å$^2$ (5) | 0.74 Å$^2$ (3) | | |

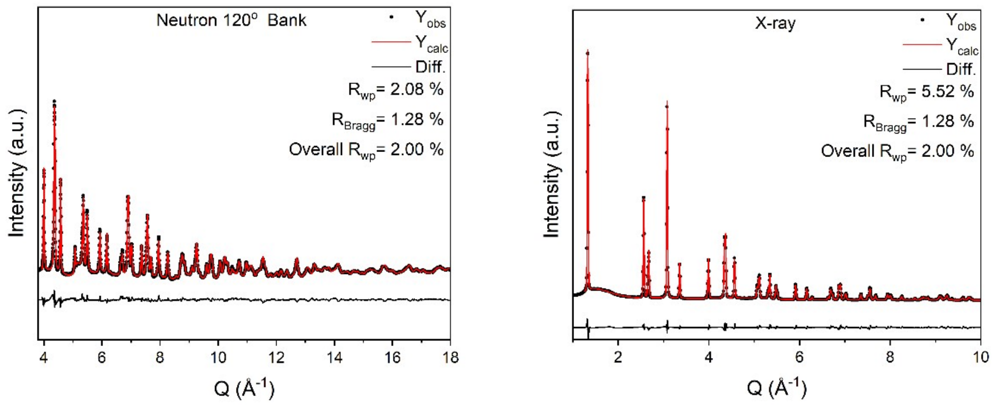


**Supplementary Figure 7**: Rietveld refinements of the neutron powder diffraction and PXRD of $LiNiO_2$ charged to 5 V and then discharged to 3 V.

**Supplementary Table 5:** Refined structural parameters for the $LiNiO_2$ charged to 5 V and discharged to 3 V.

| Space group | | | | | |
|---|---|---|---|---|---|
| R-3m | a | 2.8795 (1) Å | c | 14.223 (1) Å | |
| Atom | x | y | z | Occupancy | B |
| Li | 0 | 0 | 0 | 0.807 | 0.851 (4) Å$^2$ |
| Ni | 0 | 0 | 0 | 0.0282 (5) | 0.184 (3) Å$^2$ |
| Ni | 0 | 0 | 0.5 | 0.933 (2) | 0.184 (3) Å$^2$ |

| | | | | | |
|---|---|---|---|---|---|
| O | 0 | 0 | 0.2407 (1) | 1 | 1.107 (6) Å$^2$ |

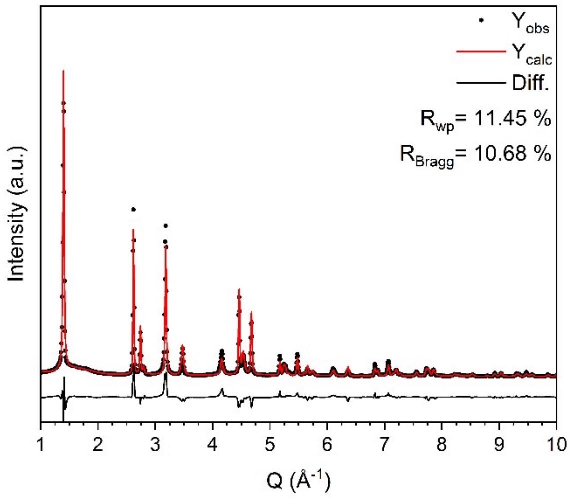


**Supplementary Figure 8**. Rietveld refinement of X-ray diffraction data including Ni in tetrahedral sites refinement for the $LiNiO_2$ charged to 4.3 V.

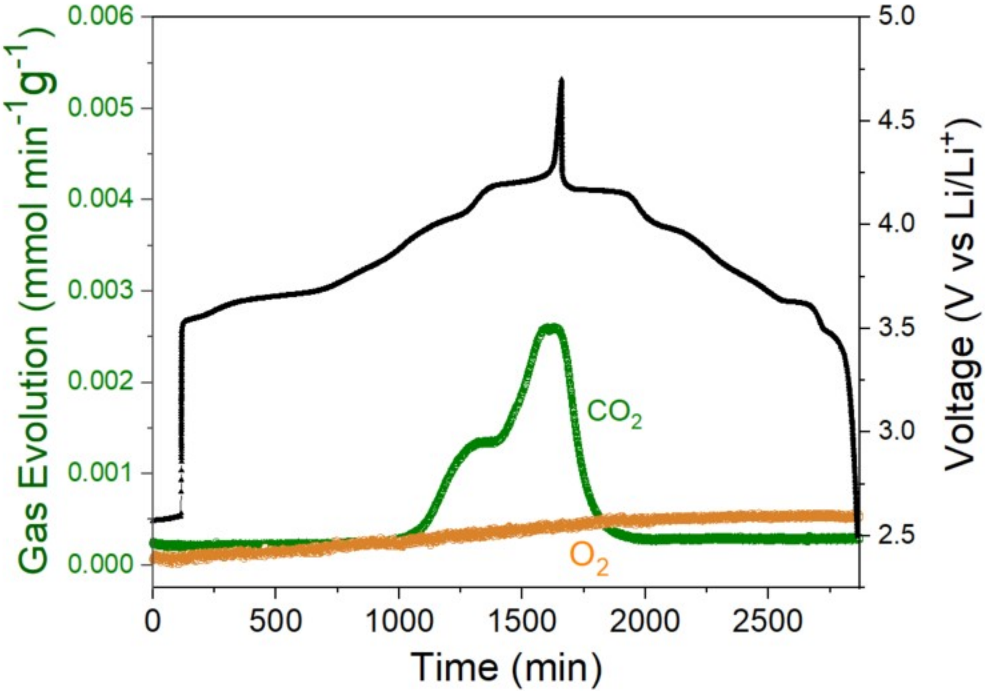


**Supplementary Figure 9:** OEMS data for the first cycle of $LiNiO_2$ cycled at a rate of 10 mA g$^{-1}$, corresponding to the charge and discharge capacity of 260.5 mAh/g and 198.7 mAh/g.

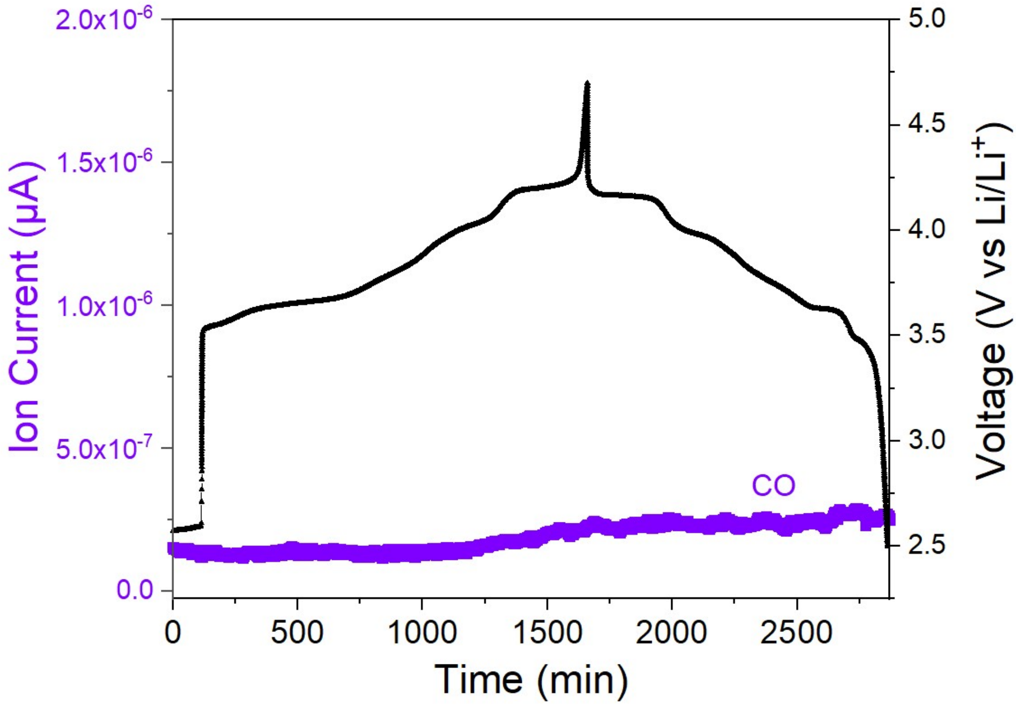


**Supplementary Figure 10:** OEMS data for the first cycle of $LiNiO_2$ cycled at a rate of 10 mA g$^{-1}$ showing no CO release.

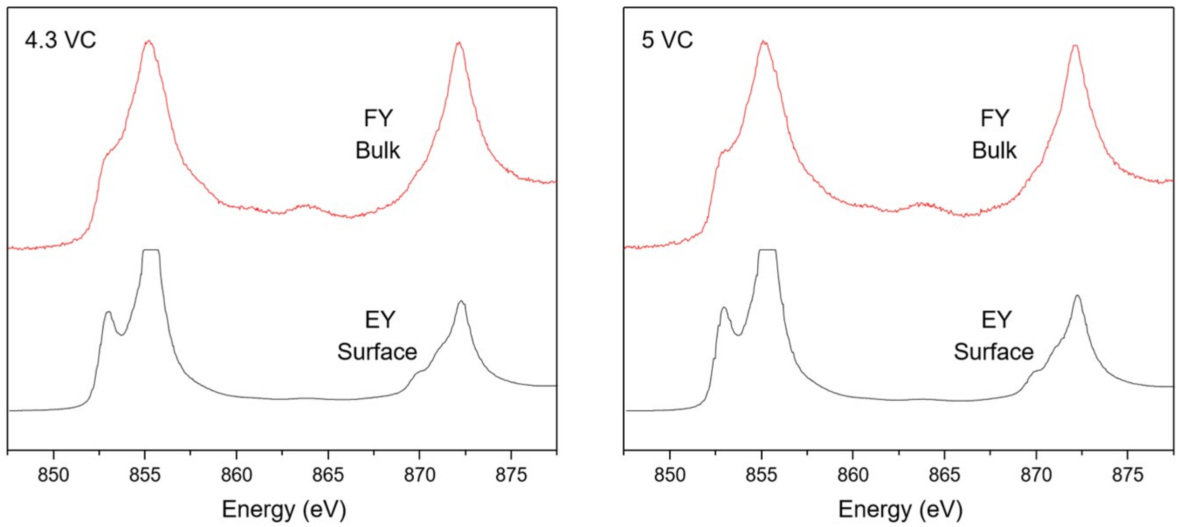


**Supplementary Figure 11.** Ni L-edge fluorescence yield (FY) and electron yield (EY) XAS data for $LiNiO_2$ charged to 4.3 V and 5 V. The peak at 853 eV is more pronounced in the EY than the FY data, indicating the presence of reduced Ni at the surface. The electron yield detector saturated during measurement, leading to truncation of the tip of the $L_{III}$ peak.

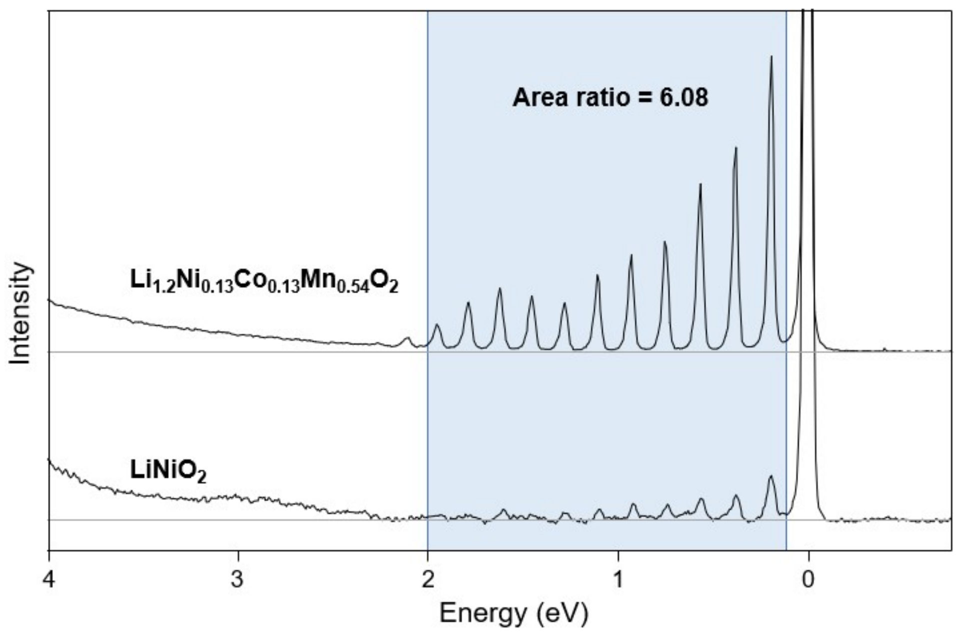


**Supplementary Figure 12.** Peak area integration of RIXS signal between 0.1 and 2 eV arising from molecular $O_2$ yielding an area ratio of 6.08.

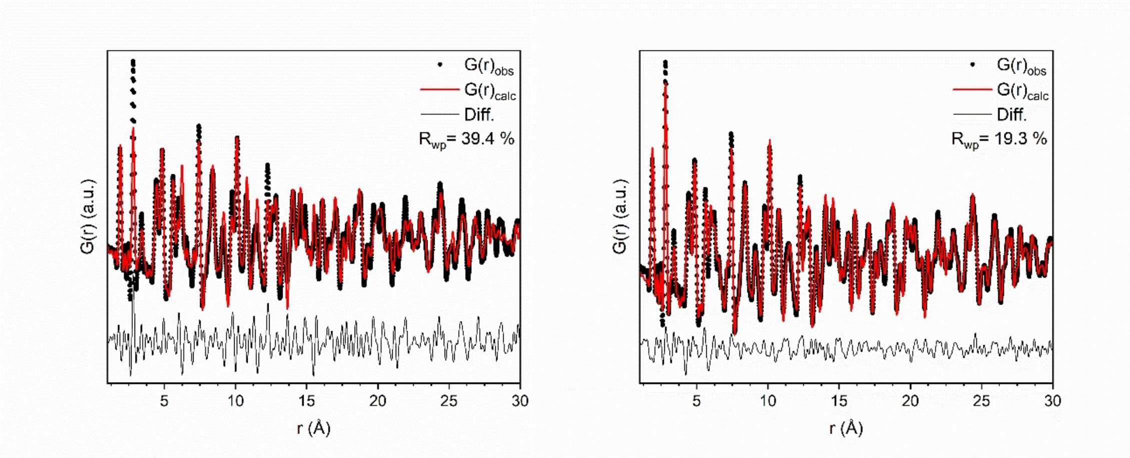


**Supplementary Figure 13:** Real space Rietveld refinements of the pair distribution function obtained from $LiNiO_2$ charged to 4.3 V. The fit on the left is done using isotropic atomic displacement parameters and the fit on the right is done using anisotropic atomic displacement parameters. In the anisotropic case, the atomic displacement parameters become twice as large along the crystallographic c-axis compared to the a/b-plane. This confirms the disorder along the stacking direction in the delithiated $LiNiO_2$ as also observe in the diffraction data and discussed in the main text.

**Supplementary Table 6**. ICP-MS results

| Sample | Ni in electrolyte after cycling (ppm) | Ni in electrolyte after first discharge (mol) | Ni in electrode film before cycling (mol) | Percentage of electrode dissolved in electrolyte (%) |
|---|---|---|---|---|
| 4.1 V | 110 | $2.64\ 10^{-7}$ | 0.111 | 0.00024 |
| 4.3 V | 104 | $2.49\ 10^{-7}$ | 0.124 | 0.00020 |
| 5 V | 132 | $3.16\ 10^{-7}$ | 0.116 | 0.00021 |
| 3VD | 147 | $3.50\ 10^{-7}$ | 0.152 | 0.00030 |

**Supplementary Table 7**. Calculated lattice parameters of $LiNiO_2$ at three different DFT setups. For comparison purposes, experimental values are reported below. See Methods for further details.

| | pristine | | fully charged (5 V) | |
|---|---|---|---|---|
| DFT setup | a (Å) | c (Å) | a (Å) | c (Å) |
| PBE+U | 2.912 | 14.434 | 2.823 | 14.932 |
| PBE+U with vdW | 2.907 | 14.364 | 2.819 | 13.358 |
| PBE with vdW | 2.884 | 14.318 | 2.827 | 13.200 |
| Experiment (this work) | 2.87785 | 14.1998 | 2.817 | 13.42 |

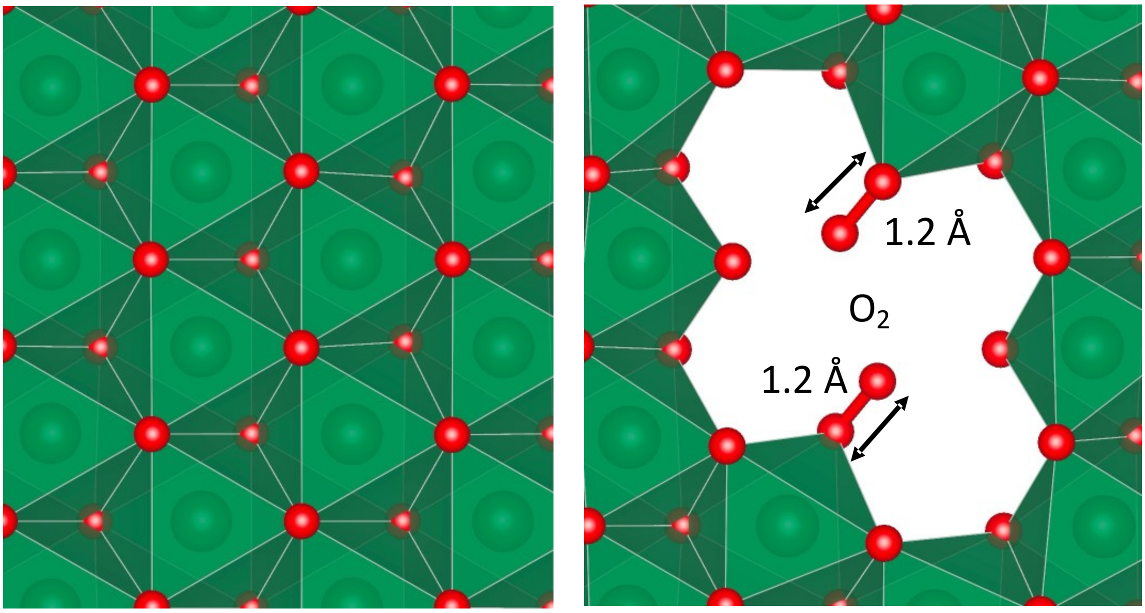


**Supplementary Figure 14:** DFT structural models for delithiated $LiNiO_2$, with and without vacancy clusters and trapped $O_2$ (right and left panels, respectively). The structure containing trapped $O_2$ was found to be more stable by 205 meV/f.u. The formation of $O_2$ from the modelling is in accord with the experimental detection of $O_2$, not $O^{2-}$ or $O^{n-}$ by RIXS.

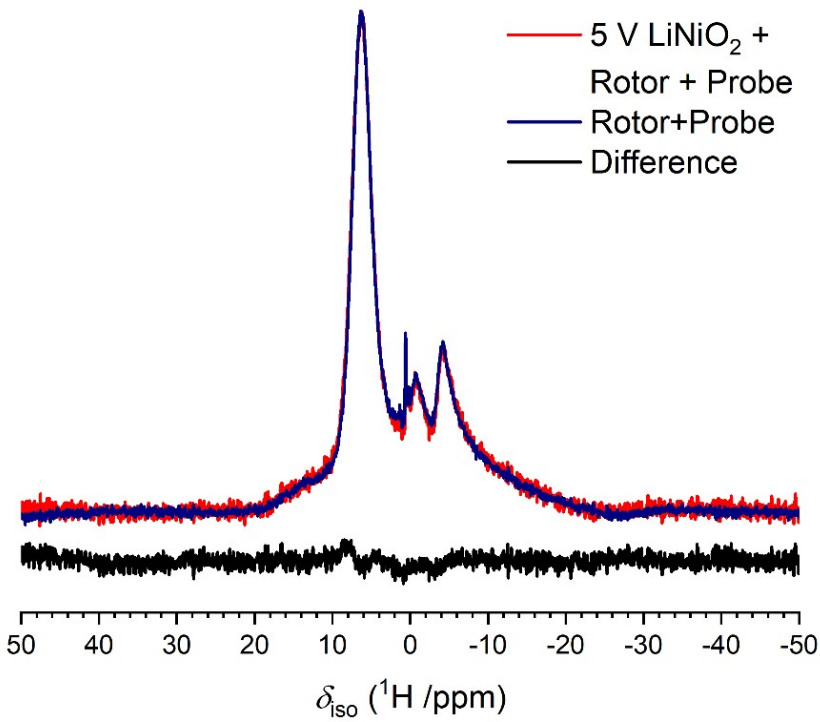


**Supplementary Figure 15.** The $^{1}H$ magic angle spinning ($\nu_R$ = 32 kHz) NMR for $LiNiO_2$ charged to 5 V(red). $H_2O$ would be observed at a shift of 4.79 ppm, however, only background signal from the rotor and probe is observed. This shows there are no detectable amounts of protons in the charged $LiNiO_2$ sample.